Ruthenium Carbene and Allenylidene Complexes Supported by the Tertiary Amine−Aromatic Diimine Ligand Set: Structural, Spectroscopic, and Theoretical Studies

Chun-Yuen Wong,*[,†] Lo-Ming Lai,[†] Chi-Yeung Lam,[†] and Nianyong Zhu[‡]

Department of Biology and Chemistry, City University of Hong Kong, Tat Chee Avenue, Kowloon, Hong Kong SAR, People's Republic of China, and Department of Chemistry, The University of Hong Kong, Pokfulam Road, Hong Kong SAR, People's Republic of China

Received June 26, 2008

Ruthenium−methoxycarbene and −allenylidene complexes bearing 1,4,7-trimethyl-1,4,7-triazacyclononane (Me_3Tacn) and 1,10-phenanthroline (phen), $[(Me_3Tacn)(phen)Ru{=}C(OMe)R]^{2+}$ (R = CH_2Ph (**1**), $CH{=}CPh_2$ (**2**), $CH{=}C(C_6H_4Cl\text{-}4)_2$ (**3**), $CH{=}C(C_6H_4Me\text{-}4)_2$ (**4**)), and $[(Me_3Tacn)(phen)Ru{=}C{=}C{=}CR_2]^{2+}$ (R = Ph (**5**), C_6H_4OMe-4 (**6**)) have been prepared. The molecular structures of **1**$(PF_6)_2$ and **2**$(PF_6)_2$ reveal Ru−C distances of 1.917(3) and 1.906(4) Å, respectively. The lowest-energy dipole-allowed absorptions for complexes **1**−**4** ($\lambda_{max} \approx 435$ nm) are assigned as $d_\pi(Ru^{II}) \rightarrow \pi^*$(phen) metal-to-ligand charge transfer (MLCT) transitions, while those for complexes **5** and **6** ($\lambda_{max} = 530$ and 585 nm, respectively) are assigned as metal-perturbed $\pi-\pi^*$ [$Ru{=}C{=}C{=}CR_2$] intraligand transitions. Complexes **1**−**4** are emissive in glassy MeOH/EtOH at 77 K: excitation at $\lambda = 430$ nm produces emission at $\lambda_{max} = 570-620$ nm, which are tentatively assigned as $d_\pi(Ru^{II}) \rightarrow \pi^*$(phen) ^{3}MLCT in nature. Density functional theory (DFT) calculations, charge decomposition analysis (CDA), and natural bond orbital (NBO) analysis on complexes **1**, **2**, **5**, and **6** suggest that allenylidene ligands are better electron donors and poorer acceptors compared with methoxycarbene ligands, and the Ru−C interactions in ruthenium−allenylidene and −methoxycarbene complexes can be depicted by the polarized formulation $Ru^{\delta+}{=}C^{\delta-}$ and nonpolarized formulation Ru=C, respectively. The methoxycarbene/allenylidene rotational barriers on **1**, **2**, and **5** are calculated to be 8.3, 6.3, and 1.5 kcal mol^{-1}, respectively.

Introduction

Ruthenium(II) complexes containing aromatic diimine ligands such as 2,2′-bipyridine (bpy) and 1,10-phenanthroline (phen) are of considerable interest because they exhibit rich photophysical and photochemical properties, which originate from the triplet $[d_\pi(Ru^{II}) \rightarrow \pi^*$(aromatic diimine)] metal-to-ligand charge transfer (^{3}MLCT) excited state. Due to the presence of the long-lived ^{3}MLCT state, $[Ru(bpy)_3]^{2+}$ and its derivatives have been a research focus in many areas including photochemistry,[1] electron transfer reactions,[2] luminescent sensing,[3] light-emitting devices,[4] and photosensitizers.[5] In the meantime, the pursuit of $[Ru(bpy)_3]^{2+}$-related complexes exhibiting desirable photophysical properties continues unabated.[6]

For ruthenium(II)−aromatic diimine complexes with general formula $[Ru(diimine)_x(L)_y]^{n+}$, their photophysical properties can be fine-tuned by controlling the energy level of the π^*(diimine) orbital via modifying the degree of conjugation in the diimine ligands. An alternative approach would be tuning the energy of the $d_\pi(Ru^{II})$ level via manipulating the Ru−L interaction. We regard ruthenium−carbon multiple bonded species bearing aromatic diimine as an interesting class of compounds because ligands such as carbene and allenylidene can interact with the metal center via π-bonding/back-bonding interaction,[7−10] and modifying the Ru−C π-interactions through varying the substituent on the ligands may yield complexes with desirable photophysical properties. In any case, understanding how the carbon-rich organic moieties perturb the electronic and photophysical properties of a [Ru(diimine)] core is an important issue for the development of functional emissive materials, although few studies were accomplished concerning this topic. Moreover, a comparison of metal−carbon bonding interaction between ruthenium−methoxycarbene and −allenylidene complexes is sparse in the literature. In this account, we have prepared a series of ruthenium−methoxycarbene and −allenylidene complexes

* Corresponding author. E-mail: acywong@cityu.edu.hk.
† City University of Hong Kong.
‡ The University of Hong Kong.

(1) (a) Kalyanasundaram, K. *Coord. Chem. Rev.* **1982**, *46*, 159. (b) Juris, A.; Balzani, V.; Barigelletti, F.; Campagna, S.; Belser, P.; von Zelewsky, A. *Coord. Chem. Rev.* **1988**, *84*, 85. (c) Balzani, V.; Barigelletti, F.; De Cola, L. *Top. Curr. Chem.* **1990**, *158*, 31. (d) Sauvage, J.-P.; Collin, J.-P.; Chambron, J.-C.; Guillerez, S.; Coudret, C.; Balzani, V.; Barigelletti, F.; De Cola, L.; Flamigni, L. *Chem. Rev.* **1994**, *94*, 993.

(2) (a) Meyer, T. J. *Acc. Chem. Res.* **1989**, *22*, 163. (b) Balzani, V.; Juris, A.; Venturi, M.; Campagna, S.; Serroni, S. *Chem. Rev.* **1996**, *96*, 759. (c) De Cola, L.; Belser, P. *Coord. Chem. Rev.* **1998**, *177*, 301.

(3) (a) Balzani, V.; Sabbatini, N.; Scandola, F. *Chem. Rev.* **1986**, *86*, 319. (b) de Silva, A. P.; Gunaratne, H. Q. N.; Gunnlaugsson, T.; Huxley, A. J. M.; McCoy, C. P.; Rademacher, J. T.; Rice, T. E. *Chem. Rev.* **1997**, *97*, 1515.

(4) (a) Lee, J.-K.; Yoo, D. S.; Handy, E. S.; Rubner, M. F. *Appl. Phys. Lett.* **1996**, *69*, 1686. (b) Elliott, C. M.; Pichot, F.; Bloom, C. J.; Rider, L. S. *J. Am. Chem. Soc.* **1998**, *120*, 6781. (c) Handy, E. S.; Pal, A. J.; Rubner, M. F. *J. Am. Chem. Soc.* **1999**, *121*, 3525. (d) Buda, M.; Kalyuzhny, G.; Bard, A. J. *J. Am. Chem. Soc.* **2002**, *124*, 6090. (e) Bernhard, S.; Barron, J. A.; Houston, P. L.; Abruna, H. D.; Ruglovksy, J. L.; Gao, X.; Malliaras, G. G. *J. Am. Chem. Soc.* **2002**, *124*, 13624.

(5) (a) O'Regan, B.; Grätzel, M. *Nature* **1991**, *353*, 737. (b) Bignozzi, C. A.; Schoonover, J. R.; Scandola, F. *Prog. Inorg. Chem.* **1997**, *44*, 1. (c) Gerfin, T.; Gratzel, M.; Walder, L. *Prog. Inorg. Chem.* **1997**, *44*, 345. (d) Kalyanasundaram, K.; Grätzel, M. *Coord. Chem. Rev.* **1998**, *177*, 347. (e) Bach, U.; Lupo, D.; Comte, P.; Moser, J. E.; Weissörtel, F.; Salbeck, J.; Spreitzer, H.; Grätzel, M. *Nature* **1998**, *395*, 583. (f) Hagfeldt, A.; Grätzel, M. *Acc. Chem. Res.* **2000**, *33*, 269. (g) D'Alessandro, D. M.; Keene, F. R. *Chem. Rev.* **2006**, *106*, 2270.

10.1021/om800592a CCC: $40.75
Publication on Web 10/22/2008

bearing 1,4,7-trimethyl-1,4,7-triazacyclononane (Me_3Tacn) and 1,10-phenanthroline (phen), and their Ru−C bonding interactions have been probed by spectroscopic means and theoretical calculations. The Me_3Tacn ligand has been chosen because (i) it is optically transparent in the UV−visible spectral region, which allows examination of the electronic transitions associated with the [(phen)Ru(carbene/allenylidene)] moiety; (ii) it is a pure σ-donor and does not compete with other ligands for π-bonding interactions. On the basis of our results, allenylidene ligands can be regarded as better electron donors and poorer acceptors compared with methoxycarbene ligands, and the Ru−C interactions in ruthenium−allenylidene and −methoxycarbene complexes can be depicted by the polarized formulation $Ru^{\delta+}=C^{\delta-}$ and nonpolarized formulation Ru=C, respectively.

Results and Discussions

Synthesis and Characterization. Methoxycarbene complexes $[(Me_3Tacn)(phen)Ru=C(OMe)R]^{2+}$ (**1**−**4**) were prepared in ca. 80% yields by reacting a Ru(II) aqua complex $[(Me_3Tacn)(phen)Ru(OH_2)]^{2+}$ with phenylacetylene or propargylic alcohols in methanol (Scheme 1). Slow diffusion of Et_2O into an acetone solution yielded analytically pure crystalline solids. They are bright yellow or orange in color, and they are sufficiently stable to be handled in air under ambient conditions in solution and solid forms. Their ^{13}C NMR spectra show low-field signals at 308.1−315.2 ppm, which are characteristic for the carbene carbon atoms.[7−11] Their ^1H signals at 4.64−4.67 ppm (s, 3H) signify the presence of the −OMe group on the

Scheme 1

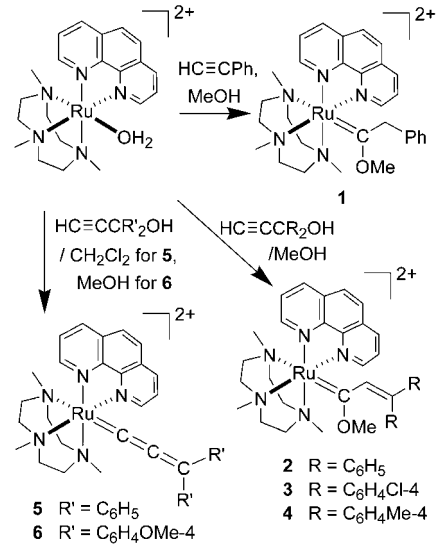

C_α. The formation of **1**−**4** might be conceived as an addition of MeOH to a transient vinylidene or allenylidene species (i.e., [Ru=C=CHR] or [Ru=C=C=CR_2]).[7−11] It is noted that (i) complex **1** features four sets of ^1H signals for the phen ligand, while the corresponding signals for complexes **2**−**4** are split into more than five sets (Figure 1); (ii) the ^{13}C NMR spectrum for **1** contains five sets of signals corresponding to Me_3Tacn, whereas those for **2**−**4** contain nine sets of Me_3Tacn signals. These findings signify that complex **1** possesses a pseudo plane of symmetry in solution on the NMR time scale at room temperature, while complexes **2**−**4** exist in locked conformations. A reasonable explanation would be the small $-CH_2Ph$ group in **1** can flip along the $C_\alpha-C_\beta$ bond, whereas the bulky $-CH=C(C_6H_4X)_2$ group in complexes **2**−**4** hampers the flipping motion due to its steric interaction with the −OMe group on C_α (Figure 1). Thus the [:C(OMe)CH_2Ph] moiety possesses a pseudo plane of symmetry, whereas [:C(OMe)CH=$C(C_6H_4X)_2$] does not. Interestingly, the two conformation-locked isomers of complex **2** coexist in the crystal structure of $\mathbf{2}(PF_6)_2\cdot(CH_3)_2CO$ (Figure 2). The argument stating that the higher Ru−C bond rotational barriers for **2**−**4** compared with that of **1** leading to the removal of the pseudo plane of symmetry for the [(Me_3Tacn)(phen)Ru] moiety on the NMR time scale has been found to be unreasonable because the methoxycarbene rotational barriers on **1** and **2** are calculated to be 8.3 and 6.3 kcal mol^{-1}, respectively (see DFT Calculations section below).

It was noted that refluxing a mixture of HC≡CC(C_6H_4OMe-4)$_2$OH and $[(Me_3Tacn)(phen)Ru(OH_2)]^{2+}$ in MeOH gave only the allenylidene complex [(Me_3Tacn)(phen)Ru=C=C=C(C_6H_4-OMe-4)$_2$]$^{2+}$ (**6**) rather than the corresponding methoxycarbene derivative [(Me_3Tacn)(phen)Ru=C(OMe)CH=C(C_6H_4OMe-4)$_2$]$^{2+}$. Another allenylidene complexes like complex **5** was prepared by reacting $[(Me_3Tacn)(phen)Ru(OH_2)]^{2+}$ with propargylic alcohols using CH_2Cl_2 as solvent. Unlike the methoxycarbene complexes, the allenylidene complexes are deep purple (for **5**) or blue (for **6**) in color and are mildly unstable upon exposure to air in solution form. Complexes **5** and **6** exhibit characteristic intense IR stretching bands at 1931 and 1946 cm^{-1}, respectively, which are comparable to the reported $\nu_{C=C=C}$ values for ruthenium−allenylidene complexes.[7−10] Interestingly, the ^1H NMR signal for the NCH_3 trans to the C_α is sensitive to the change of ligand from [:C(OMe)R] to [:C=C=CR_2] (**1**−**4**, 1.41−1.48 ppm; **5** and **6**, 2.52−2.59 ppm), suggesting that the

(6) (a) Sykora, M.; Kincaid, J. R. *Nature* **1997**, *387*, 162. (b) Beer, P. D.; Szemes, F.; Balzani, V.; Salà, C. M.; Drew, M. G. B.; Dent, S. W.; Maestri, M. *J. Am. Chem. Soc.* **1997**, *119*, 11864. (c) Farzad, F.; Thompson, D. W.; Kelly, C. A.; Meyer, G. J. *J. Am. Chem. Soc.* **1999**, *121*, 5577. (d) Gao, F. G.; Bard, A. J. *J. Am. Chem. Soc.* **2000**, *122*, 7426. (e) Nazeeruddin, M. K.; Péchy, P.; Renouard, T.; Zakeeruddin, S. M.; Humphry-Baker, R.; Comte, P.; Liska, P.; Cevey, L.; Costa, E.; Shklover, V.; Spiccia, L.; Deacon, G. B.; Bignozzi, C. A.; Grätzel, M. *J. Am. Chem. Soc.* **2001**, *123*, 1613. (f) Galoppini, E.; Guo, W.; Zhang, W.; Hoertz, P. G.; Qu, P.; Meyer, G. J. *J. Am. Chem. Soc.* **2002**, *124*, 7801. (g) Zhan, W.; Alvarez, J.; Crooks, R. M. *J. Am. Chem. Soc.* **2002**, *124*, 13265. (h) Potvin, P. G.; Luyen, P. U.; Bräckow, J. *J. Am. Chem. Soc.* **2003**, *125*, 4894. (i) Kalyuzhny, G.; Buda, M.; McNeill, J.; Barbara, P.; Bard, A. J. *J. Am. Chem. Soc.* **2003**, *125*, 6272. (j) Welter, S.; Brunner, K.; Hofstraat, J. W.; De Cola, L. *Nature* **2003**, *421*, 54. (k) Dunn, A. R.; Belliston-Bittner, W.; Winkler, J. R.; Getzoff, E. D.; Stuehr, D. J.; Gray, H. B. *J. Am. Chem. Soc.* **2005**, *127*, 5169. (l) McFarland, S. A.; Lee, F. S.; Cheng, K. A. W. Y.; Cozens, F. L.; Schepp, N. P. *J. Am. Chem. Soc.* **2005**, *127*, 7065. (m) Soltzberg, L. J.; Slinker, J. D.; Flores-Torres, S.; Bernards, D. A.; Malliaras, G. G.; Abruña, H. D.; Kim, J.-S.; Friend, R. H.; Kaplan, M. D.; Goldberg, V. *J. Am. Chem. Soc.* **2006**, *128*, 7761. (n) Johansson, E.; Zink, J. I. *J. Am. Chem. Soc.* **2007**, *129*, 14437. (o) McGee, K. A.; Veltkamp, D. J.; Marquardt, B. J.; Mann, K. R. *J. Am. Chem. Soc.* **2007**, *129*, 15092.

(7) Bruce, M. I. *Chem.Rev.* **1998**, *98*, 2797.

(8) Cadierno, V.; Gamasa, M. P.; Gimeno, J. *Eur. J. Inorg. Chem.* **2001**, 571.

(9) *Coord. Chem. Rev.* **2004**, *248*, 1531−1715.

(10) Che, C.-M.; Ho, C.-M.; Huang, J.-S. *Coord. Chem. Rev.* **2007**, *251*, 2145.

(11) (a) Consiglio, G.; Morandini, F.; Ciani, G. F.; Sironi, A. *Organometallics* **1986**, *5*, 1976. (b) Pilette, D.; Ouzzine, K.; Bozec, H. L.; Dixneuf, P. H.; Rickard, C. E. F.; Roper, W. R. *Organometallics* **1992**, *11*, 809. (c) Gamasa, M. P.; Gimeno, J.; González-Bernardo, C.; Borge, J.; García-Granda, S. *Organometallics* **1997**, *16*, 2483. (d) Bianchini, C.; Mantovani, N.; Marchi, A.; Marvelli, L.; Masi, D.; Peruzzini, M.; Rossi, R.; Romerosa, A. *Organometallics* **1999**, *18*, 4501. (e) Esteruelas, M. A.; Gómez, A. V.; López, A. M.; Oliván, M.; Oñate, E.; Ruiz, N. *Organometallics* **2000**, *19*, 4. (f) Hansen, H. D.; Nelson, J. H. *Organometallics* **2000**, *19*, 4740. (g) Weberndörfer, B.; Werner, H. *J. Chem. Soc., Dalton Trans.* **2002**, 1479. (h) Ghebreyessus, K. Y.; Nelson, J. H. *Inorg. Chim. Acta* **2003**, *350*, 12. (i) Asensio, A.; Buil, M. L.; Esteruelas, M. A.; Oñate, E. *Organometallics* **2004**, *23*, 5787. (j) Demerseman, B.; Toupet, L. *Eur. J. Inorg. Chem.* **2006**, 1573. (k) Wong, C.-Y.; Man, W.-L.; Wang, C.; Kwong, H.-L.; Wong, W.-Y.; Lau, T.-C. *Organometallics* **2008**, *27*, 324.

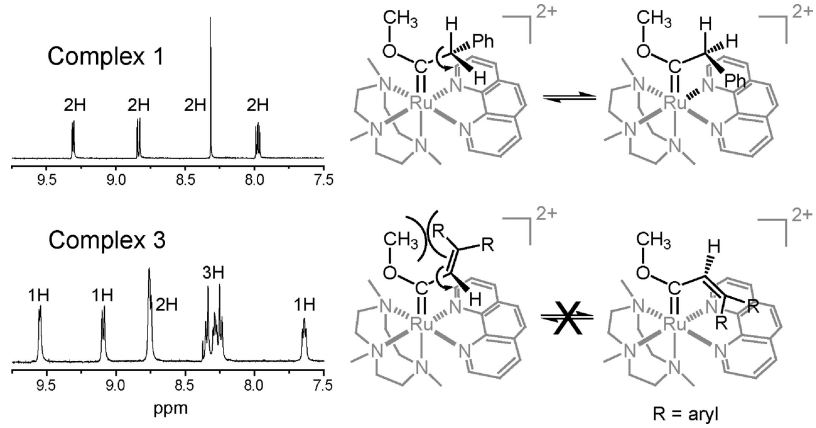

Figure 1. ^{1}H NMR spectra showing the signals for the phen ligand of complexes **1** and **3**, and schematic showing the flipping motion along the $C_\alpha-C_\beta$ bonds in complexes **1**−**4**.

Ru−C bonding interactions in Ru−methoxycarbene and −allenylidene complexes are different.

Crystal Structures. The molecular structures of $\mathbf{1}(PF_6)_2\cdot(CH_3)_2CO$ and $\mathbf{2}(PF_6)_2\cdot(CH_3)_2CO$ have been determined by X-ray crystallography. Perspective views of the complex cations are shown in Figure 2. In each case, the Ru atom adopts a distorted octahedral geometry, with the Me_3Tacn facially coordinating to it. The short Ru−C_α distances [**1**, 1.917(3); **2**, 1.906(4) Å], together with the angles around the C_α atoms (which are consistent with sp^2 hybridization), reveal the presence of ruthenium−carbon multiple-bonding character. These Ru−C_α distances are shorter than those for arene/phosphine-supported derivatives bearing [:C(OMe)CH_2Ph] or [:C(OMe)CH=CPh_2] moieties. For example, Ru−C_α distances in $[Cp(Ph_2PCH(CH_3)CH_2PPh_2)Ru{=}C(OMe)CH_2Ph]^+$,[11a] $[(\eta^6\text{-}1,2,4\text{-}Me_3C_6H_2\text{-}5\text{-}CH_2CH_2CH_2PPh_2(Cl)Ru{=}C(OMe)CH_2Ph]^+$,[11h] $[(\eta^6\text{-}C_6Me_6)(PR_3)(Cl)Ru{=}C(OMe)CH_2Ph]^+$,[11f] $[(\eta^6\text{-}1,2,4\text{-}Me_3C_6H_2\text{-}5\text{-}CH_2CH_2CH_2PPh_2(Cl)Ru(=C(OMe)CH=CPh_2]^+$,[11h] and $[(C_6H_6)(PMe_3)(Cl)Ru{=}C(OMe)CH{=}CPh_2]^+$ [11b] are 1.93(2)−1.994(19) Å. As the bonding interaction of heteroatom-stabilized carbenes are generally represented by the mesomeric structures [M=C−OR] ↔ [M^-−C^+−OR] ↔ [M^-−C=O^+R],[12] the shorter Ru−C_α distances in **1** and **2** are in accordance with the stronger electron-donating effect of the (Me_3Tacn)(phen) ligand set compared with that of phosphine/arene, which destabilizes the latter two mesomeric forms to a greater extent and gives a stronger Ru−C π-interaction. It is noted that the Ru−N_{Tacn} distances are not equivalent: $\Delta[(Ru-N_{trans}) - (Ru-N_{cis})_{avergae}]$ are 0.047 and 0.064 Å for **1** and **2**, respectively. This trans influence is brought about by the Ru−C multiple-bonding interaction. Interestingly, the Ru−$N_{Tacn\text{-}trans}$ distances for **1** and **2** are 0.054−0.063 Å longer than that in the dicationic complex $[(Me_3Tacn)(bpy)Ru{=}O]^{2+}$ (2.183(6) Å, bpy = 2,2′-bipyridine).[13] This reveals that the structural trans influence of [:C(OMe)CH_2Ph] or [:C(OMe)CH=CPh_2] moieties is stronger than that of the oxo ligand.

Absorption Spectroscopy. The UV−visible spectral data of complexes **1**−**6** are summarized in Table 1, and their absorption spectra are depicted in Figure 3. All the complexes exhibit intense high-energy absorption at $\lambda_{max} \le 300$ nm ($\varepsilon_{max} \ge 10^4$ dm^3 mol^{-1} cm^{-1}). Methoxycarbene complexes **1**−**4** show moderately intense bands at $\lambda_{max} \approx 435$ nm ($\varepsilon_{max} = (3-6) \times 10^3$ dm^3 mol^{-1} cm^{-1}) as their lowest-energy electronic transition. In the literature, ruthenium(II) complexes bearing aromatic diimine ligands such as $[Ru(bpy)_3]^{2+}$ and $[Ru(phen)_3]^{2+}$ feature two types of characteristic absorption bands: highly intense absorptions in the UV region, which are attributed to the diimine intraligand $\pi \rightarrow \pi^*$ transitions, and moderately intense absorptions in the visible region, which are ascribed to $d_\pi(Ru^{II}) \rightarrow \pi^*$(diimine) metal-to-ligand charge transfer (MLCT) transitions.[1d] In this work, the lowest-energy absorptions at $\lambda_{max} \approx 435$ nm ($\varepsilon_{max} = (3-6) \times 10^3$ dm^3 mol^{-1} cm^{-1}) for methoxycarbene complexes **1**−**4** are assigned as $d_\pi(Ru^{II}) \rightarrow \pi^*$(diimine) metal-to-ligand charge transfer (MLCT) transitions. The alternative assignment for the visible absorptions to $d_\pi(Ru^{II}) \rightarrow \pi^*$(carbene) is unreasonable because the absorption maxima are not sensitive to the change of carbene ligand from [:C(OMe)CH_2Ph] to [:C(OMe)CH=$C(C_6H_4X\text{-}4)_2$] or the change of substituents X on the [:C(OMe)CH=$C(C_6H_4X\text{-}4)_2$] moiety.

The absorption profiles for allenylidene complexes **5** and **6** are noticeably different from those of **1**−**4**. They display intense low-energy absorption at 530 and 585 nm, respectively ($\varepsilon_{max} \ge 10^4$ dm^3 mol^{-1} cm^{-1}). As complexes **1**−**4** show no strong absorption at $\lambda > 500$ nm, the intense low-energy absorption band for **5** and **6** is likely to originate from the [Ru=C=C=$C(C_6H_4X\text{-}4)_2$] moiety. Such absorption red-shifts in energy as the electron-donating ability of the C_6H_4X-4 ring increases, revealing that the transition possesses some allenylidene-to-ruthenium ligand-to-metal charge transfer (LMCT) character. This finding is consistent with previous spectroscopic studies on allenylidene complexes *trans*-$[(16\text{-TMC})ClRu{=}C{=}C{=}C(C_6H_4X\text{-}4)_2]^+$ (16-TMC = 1,5,9,13-tetramethyl-1,5,9,13-tetraazacyclohexadecane) and *trans*-$[(dppm)ClM{=}C{=}C{=}C(C_6H_4X\text{-}4)_2]^+$ (M = Ru, Os, dppm = bis(diphenylphosphino)methane), in which their lowest-energy intense absorption bands at $\lambda_{max} = 479-527$ nm are metal-perturbed [Ru=C=C=CR_2] $\pi \rightarrow \pi^*$ intraligand transition with some allenylidene-to-metal LMCT character.[14,15] The red-shift of the absorption maximum for $[(Me_3Tacn)(phen)Ru{=}C{=}C{=}C(C_6H_4X\text{-}4)_2]^{2+}$ (530 nm, X = H; 585 nm, X = OMe) compared with that of *trans*-$[(16\text{-TMC})ClRu{=}C{=}C{=}C(C_6H_4X\text{-}4)_2]^+$ (479 nm, X = H; 513 nm, X = OMe) is consistent with the fact that the dicationic $[(Me_3Tacn)(phen)Ru]^{2+}$ carries more

(12) (a) Schubert, U. *Transition Metal Carbene Complexes*; Verlag Chemie: Weinheim, Germany, 1983; p 113. (b) Collman, J. P.; Hegedus, L. S.; Norton, J. R.; Finke, R. G. *Principles and Applications of Organotransition Metal Chemistry*; University Science Books: Mill Valley, CA, 1987; p 119.

(13) Cheng, W.-C.; Yu, W.-Y.; Cheung, K.-K.; Che, C.-M. *J. Chem. Soc., Dalton Trans.* **1994**, 57.

(14) Wong, C.-Y.; Che, C.-M.; Chan, M. C. W.; Leung, K.-H.; Phillips, D. L.; Zhu, N. *J. Am. Chem. Soc.* **2004**, *126*, 2501.

(15) Wong, C.-Y.; Tong, G. S. M.; Che, C.-M.; Zhu, N. *Angew. Chem., Int. Ed.* **2006**, *45*, 2694.

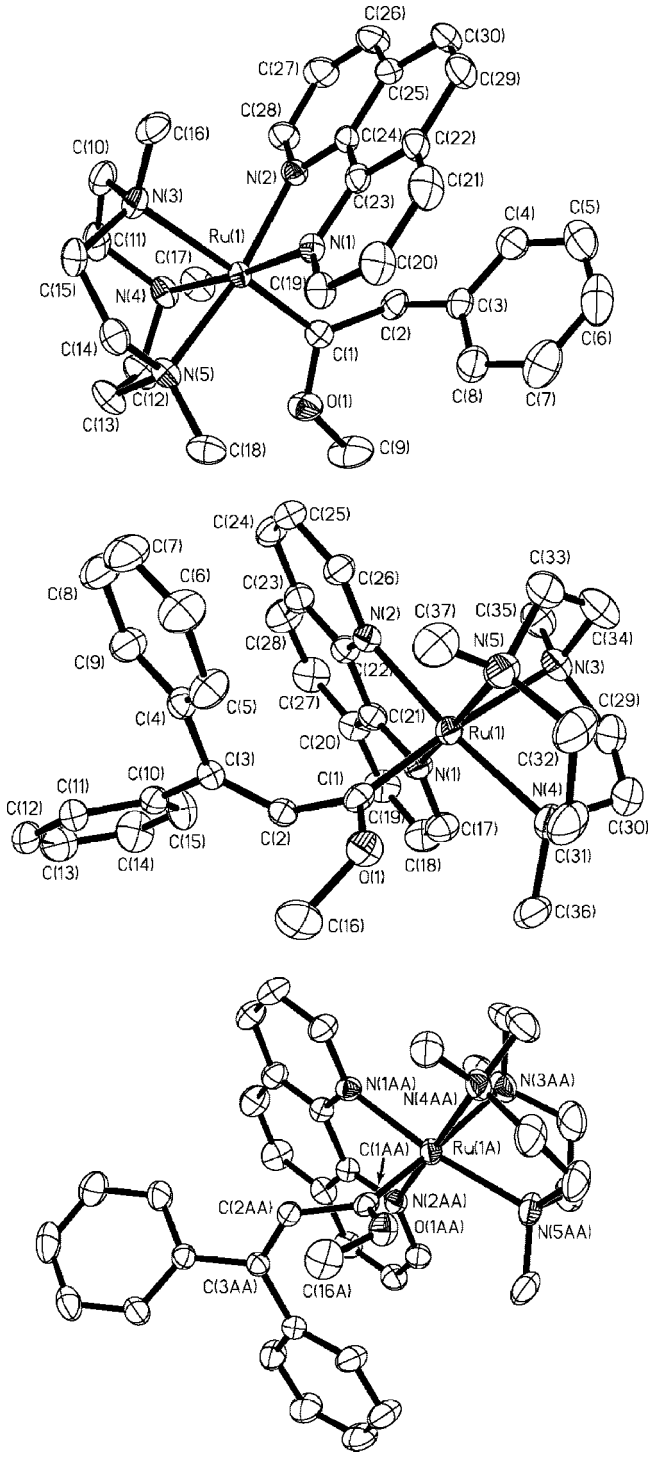

Figure 2. Perspective views of the cation in $\mathbf{1}(PF_6)_2 \cdot (CH_3)_2CO$ (top) and the two conformers in $\mathbf{2}(PF_6)_2 \cdot (CH_3)_2CO$ (middle and bottom, thermal ellipsoids are drawn at 30% probability). Selected bond lengths (Å) and angles (deg): **1**: Ru(1)−C(1) 1.917(3), C(1)−C(2) 1.523(4), C(2)−C(3) 1.513(4), C(1)−O(1) 1.333(4), mean Ru(1)−N_{phen} 2.108, mean Ru(1)−$N_{Tacn\text{-}cis}$ 2.190, Ru(1)−$N_{Tacn\text{-}trans}$ 2.237(2), Ru(1)−C(1)−C(2) 126.3(2), Ru(1)−C(1)−O(1) 118.4(2), C(1)−Ru(1)−N(3) 174.25(11). **2**: Ru(1)−C(1) 1.906(4), C(1)−C(2) 1.499(5), C(2)−C(3) 1.323(5), C(1)−O(1) 1.345(5), mean Ru(1)−N_{phen} 2.118, mean Ru(1)−$N_{Tacn\text{-}cis}$ 2.182, Ru(1)−$N_{Tacn\text{-}trans}$ 2.246(4), Ru(1)−C(1)−C(2) 123.1(3), Ru(1)−C(1)−O(1) 122.4(3), C(1)−Ru(1)−N(3) 175.12(15).

electronic charge, and its π-accepting ligand phen can further lower the energy level of the metal center.

Table 1. UV−Visible Absorption Data for Complexes 1−6 in CH_3CN at 298 K

complex	λ_{max}/nm (ε_{max}/dm^3 mol^{-1} cm^{-1})
1	263 (22 520), 295 (sh, 13 020), 354 (3880), 434 (3740)
2	254 (34 410), 297 (sh, 16 520), 435 (3720)
3	257 (31 540), 295 (sh, 14 260), 435 (2990)
4	254 (33 200), 295 (sh, 16 900), 435 (5400)
5	270 (34 860), 294 (sh, 15 820), 342 (7350), 434 (sh, 4570), 530 (13 420)
6	268 (32 110), 296 (sh, 11 950), 355 (5650), 411 (19 110), 585 (18 490)

Methoxycarbene ligands are generally characterized as a type of Fischer carbene, which interact with low-valent metal centers via σ-bonding and π-back-bonding. This bonding description is apparently true for the Ru−C bonding interaction in complexes **1**−**4** because their $d_\pi(Ru^{II}) \rightarrow \pi^*$(diimine) MLCT transitions are insensitive to the change of conjugation/substituent on the carbene ligands; that is, no strong Ru−C π-interaction is operating. Although the energy of the $d_\pi(Ru^{II}) \rightarrow \pi^*$(diimine) MLCT transitions associated with the $[(Me_3Tacn)(phen)Ru(L)]^{2+}$ would be an excellent probe to compare the Ru−C π-interaction in methoxycarbene and allenylidene complexes, the absorption spectra for the allenylidene complexes are complicated by the intense metal-perturbed $[Ru{=}C{=}C{=}CR_2]$ $\pi \rightarrow \pi^*$ intraligand transition. This drives us to investigate the Ru−C π-interactions via theoretical calculations (see DFT Calculations section below).

Emission Spectroscopy. Methoxycarbene complexes **1**−**4** are not emissive in solution at room temperature, but they emit in glassy MeOH/EtOH (1:3, v/v; 77 K) solution. Allenylidene complexes **5** and **6** are not emissive in both conditions. Excitation of **1** at $\lambda = 430$ nm gives emission at $\lambda_{max} = 570$ nm, while exciting **2**−**4** at the same energy gives essentially the same emission spectra with $\lambda_{max} = 620$ nm (Figure 4). The

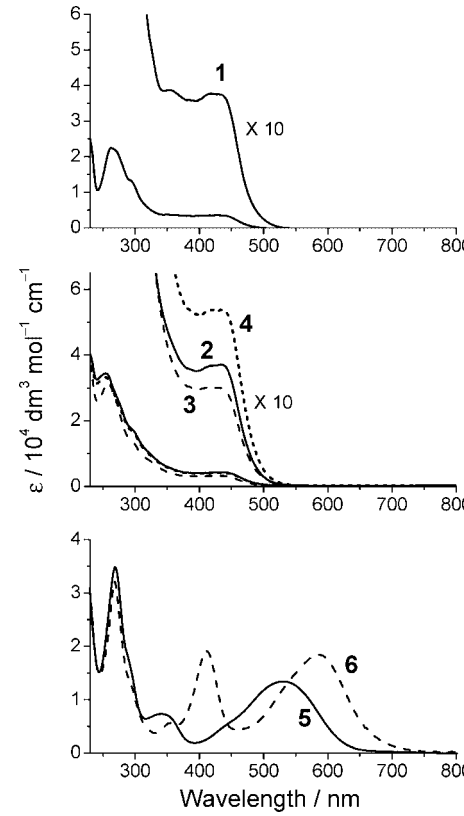

Figure 3. UV−visible absorption spectra of **1**−**6** in CH_3CN at 298 K.

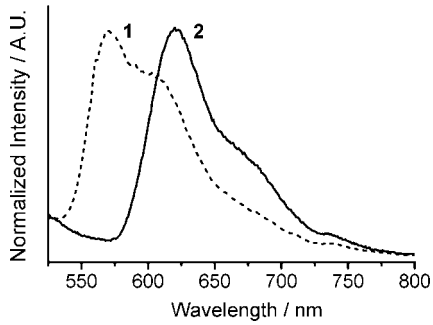

Figure 4. Glass emission spectra of **1** and **2** in MeOH/EtOH (1:3, v/v; 77 K; λ_{ex} = 430 nm).

emission lifetimes for these complexes are shorter than 0.1 μs. These emissions are tentatively ascribed as $d_\pi(Ru^{II}) \rightarrow \pi^*$(phen) ^{3}MLCT in nature. This assignment is supported by the following findings: (1) changing the substituents X on [:C(OMe)CH=C(C$_6$H$_4$X-4)$_2$] has little influence on the emission energies of complexes **2**−**4**; (2) the emission energy for **1** is higher than the $d_\pi(Ru^{II}) \rightarrow \pi^*$(polypyridine) ^{3}MLCT emission energies for [(tpy)(bpy)Ru=C(OMe)CH$_2$R]$^{2+}$ (597 and 615 nm for R = C$_6$H$_4$OMe-4 and *t*-Bu respectively; tpy = 2,2′:6′,2″-terpyridine),[16] which parallels the trend that the energy of the π^*(phen) orbital is higher than that of π^*(tpy). The nonemissive nature of **1**−**4** at room temperature suggests the presence of nonradiative pathways of deactivation of the lowest-lying $d_\pi(Ru^{II}) \rightarrow \pi^*$(polypyridine) ^{3}MLCT excited state, which may be attributed to the nonrigid structure of the methoxycarbene ligands in solution (DFT calculations suggest that the rotational barriers for the methoxycarbene ligands on **1** and **2** are 8.3 and 6.3 kcal mol^{-1}, respectively). Allenylidene complexes **5** and **6** are not emissive because their lowest-lying excited states are not the $d_\pi(Ru^{II}) \rightarrow \pi^*$(polypyridine) ^{3}MLCT state.

DFT Calculations. The ground-state structures of the complexes **1**, **2**, **5**, and **6** were optimized at the DFT level (PBE1PBE).[17] The PBE1PBE functional was employed because it had been used to calculate ruthenium(II)−acetylide[18] and −alkoxycarbene[11k] systems, and satisfactory results had been obtained. Frequency calculations were also performed on all the optimized complexes. As no imaginary vibrational frequencies were encountered, the optimized stationary points were confirmed to be local minima. Table 2 summarizes the compositions of the highest-occupied molecular orbitals (HOMOs) and the lowest-unoccupied molecular orbitals (LUMOs) for the calculated complexes, and Figure 5 depicts the plots of the HOMOs and LUMOs (see Supporting Information for detailed optimized structural data, orbital energies/compositions, and calculated frequencies). It would be worthwhile to note that (1) the HOMO−LUMO gaps for methoxycarbene complexes **1** and **2** are larger than those for allenylidene complexes **5** and **6** (by at least 0.5 eV), although both types of complexes possess ruthenium−carbon double-bond formalism; (2) changing the methoxycarbene ligand from [:C(OMe)CH$_2$Ph] to [:C(OMe)-CH=CPh$_2$] can decrease the HOMO−LUMO gap by about 0.5 eV; (3) the HOMOs and LUMOs for the allenylidene complexes are delocalized along the [Ru=C=C=CR$_2$] moiety, while those for the methoxycarbene complexes are localized on the [Ru=C(OMe)R] and phen, respectively. All these findings suggest that the frontier orbitals of [(Me$_3$Tacn)(phen)RuL]$^{2+}$ (L = methoxycarbene/allenylidene) are sensitive to the Ru−C bonding interaction.

A simple way to compare the π-accepting ability of methoxycarbene and allenylidene ligands is to evaluate their ability to stabilize/destabilize the d_π orbitals of the ruthenium center. Defining the direction along the Ru−C as the *z*-axis and the axis bisecting the phen ligand as the *x*-axis, the d_π orbitals are linear combinations of d_{xz}, d_{yz}, and d_{x2-y2} orbitals (d_{x2-y2} orbital is involved as the plane of phen is not perfectly perpendicular to the *z*-axis). Figure 6 depicts a plot of the energies of the d_π orbitals for **1**, **5**, and their corresponding frozen [(Me$_3$Tacn)(phen)Ru]$^{2+}$ fragments. It is found that the d_π orbitals of the [(Me$_3$Tacn)(phen)Ru]$^{2+}$ fragments are destabilized to a greater extent by allenylidene compared with methoxycarbene, suggesting that allenylidene ligands are poorer π-acceptors. The charge decomposition analysis (CDA)[19] for the interactions between the closed-shell fragments [(Me$_3$Tacn)(phen)Ru]$^{2+}$ and [:C(OMe)R] or [:C=C=CR$_2$] also supports this finding (Table 3). As the residue terms (Δ) are essentially zero, the Ru−methoxycarbene and −allenylidene complexes in this work can be discussed within the framework of the Dewar−Chatt−Duncanson donor−acceptor model. The ratio of the values for [(Me$_3$Tacn)(phen)Ru]$^{2+}$ → [C(OMe)R] or [C=C=CR$_2$] back-donation (*b*) and [C(OMe)R] or [C=C=CR$_2$] → [(Me$_3$Tacn)(phen)Ru]$^{2+}$ donation (*d*), *b*/*d*, would reflect the relative weighting of these two bonding modes: the *b*/*d* ratios are 0.559−0.638 and 0.279−0.317 for methoxycarbene and allenylidene complexes, respectively. This reveals that (1) both the methoxycarbene and allenylidene ligands are stronger electron donors than electron acceptors; (2) allenylidene ligands are better electron donors and poorer electron acceptors compared with methoxycarbene ligands.

Natural bond orbital (NBO)[20] analysis has also been performed on the calculated complexes in order to examine the charge distribution along the [Ru=C(OMe)R] and [Ru=C=C=CR$_2$] moieties (Table 4). It is noted that the Ru−C bonds in the carbene complexes are less polarized compared with those in allenylidene complexes: the natural charge differences between Ru and C$_\alpha$, i.e., Charge(Ru) − Charge(C$_\alpha$), are essentially zero for **1** and **2** (−0.02 and 0.01, respectively), whereas they are 0.37 and 0.39 for **5** and **6**, respectively. These natural charge distributions suggest that it may be appropriate to consider a polarized formulation, $Ru^{\delta+}=C^{\delta-}$, for ruthenium−allenylidene complexes and a relative nonpolarized formulation, Ru=C, for ruthenium−methoxycarbene complexes. Although the bonding interaction in metal−allenylidene complexes is generally represented by the cumulene and alkyne mesomeric forms [M^n=C=C=CR$_2$] ↔ [M^{n-1}−C$^+$=C=CR$_2$] ↔ [M^{n-1}−C≡C−C$^+$R$_2$], one should not jump to the conclusion that the M−C$_\alpha$ bonds in allenylidene complexes are polarized in a $Ru^{\delta-}=C^{\delta+}$ manner. This is because (1) no prior knowledge on the real/absolute charge distribution along the M=C=C=CR$_2$ moiety is given or implied by the mesomeric forms, thus it is not correct to state that metal centers carry negative charge and C$_\alpha$ carries a positive charge based on the [M^{n-1}−C$^+$=C=CR$_2$] mesomeric form, and (2) previous MP2 calculations on [Cl(NH$_3$)$_4$Ru=C=C=CPh$_2$]$^+$ and DFT calculations on [Cl(PH$_3$)$_4$Ru=C=C=CH$_2$]$^+$ also revealed that the Ru centers

(16) Wong, C.-Y.; Chan, M. C. W.; Zhu, N.; Che, C.-M. *Organometallics* **2004**, *23*, 2263.
(17) (a) Perdew, J. P.; Burke, K.; Ernzerhof, M. *Phys. Rev. Lett.* **1996**, *77*, 3865. (b) Adamo, C.; Barone, V. *J. Chem. Phys.* **1999**, *110*, 6158.
(18) Wong, C.-Y.; Che, C.-M.; Chan, M. C. W.; Han, J.; Leung, K.-H.; Phillips, D. L.; Wong, K.-Y.; Zhu, N. *J. Am. Chem. Soc.* **2005**, *127*, 13997.
(19) (a) Frenking, G.; Fröhlich, N. *Chem. Rev.* **2000**, *100*, 717. (b) Dapprich, S.; Frenking, G. *J. Phys. Chem.* **1995**, *99*, 9352.
(20) Reed, A. E.; Curtiss, L. A.; Weinhold, F. *Chem. Rev.* **1988**, *88*, 899.

Table 2. HOMO and LUMO Compositions of $[(Me_3Tacn)(Phen)Ru(L)]^{2+}$

			% composition			
L	HOMO−LUMO gap/eV	molecular orbital	Ru	C(OMe)R/C=C=CR_2	Phen	Me_3Tacn
:C(OMe)CH_2Ph	4.108	HOMO	49.81	30.13	15.22	4.84
		LUMO	8.57	0.79	83.03	7.62
:C(OMe)CH=CPh_2	3.621	HOMO	36.15	50.96	9.16	3.74
		LUMO	11.34	0.96	75.40	12.30
:C=C=CPh_2	3.148	HOMO	56.38	28.97	8.06	6.58
		LUMO	24.66	63.00	5.44	6.89
:C=C=C(C_6H_4OMe-4)$_2$	3.102	HOMO	44.75	46.58	4.16	4.50
		LUMO	20.50	67.26	5.82	6.42

are more positive than C_α in terms of Mulliken or natural charge.[14,21] Interestingly, NBO analysis on $[(Cl)(NO)(PH_3)$-Re=C=C=C=C=Re$(PH_3)(NO)(Cl)]^{2+}$ at the Hartree−Fock level also revealed that the C_4 unit is negatively charged compared with the two Re centers, suggesting the $Re^{\delta+}$=$C^{\delta-}$ polarized formulation.[22]

The dihedral angles between the Ru−C_α−O and N(1)−Ru−C_α planes for **1** and **2** in the crystal structures are 118.1° and 139.6°, respectively, whereas they are 145.1° and 138.6°, respectively, in the fully optimized gas-phase structures for **1** and **2** at the DFT level. For complexes in octahedral geometry, the concerned dihedral angle close to 0° or a multiple of 90° in principle allows maximization of the M−L π-interaction and leads to lower orbital energies, and a deviation from these values implies the presence of steric factors. To gain further insight into the conformational landscape, relaxed potential energy surface scans as a function of the concerned dihedral angles for **1** and **2** have been carried out: the dihedral angles are rotated through 360° with 10° resolution and with geometry optimization at each step. Figure 7 depicts the plots of energy as a function of the dihedral angle. It is noted that points with the dihedral angles of ca. 0°, 90°, 180°, and 270° in the plots are not local minima, whereas the peak maxima correspond to geometries in which the −OMe, −CH_2Ph/−CH=CPh_2 groups on the carbene ligands pointing toward the −Me groups on Me_3Tacn. This reveals that the rotational barriers for **1** and **2** are dominated by intramolecular steric factors, and the optimized geometries vary due to electronic and steric effects. The rotational barriers for the methoxycarbenes complexes **1** and **2** are found to be 8.3 and 6.3 kcal mol^{-1}, respectively. These energies are within the range of previously calculated rotational barrier for late transition metal carbene complexes (ca. 6−12 kcal mol^{-1}).[23] These low rotational barriers reflect the nonrigid structure of the methoxycarbene ligands in solution and provide a nonradiative deactivation pathway of the lowest-lying $d_\pi(Ru^{II})$ → π^*(polypyridine) ^{3}MLCT excited state. Interestingly, the rotational barrier for the allenylidene on **5** is calculated to be only 1.5 kcal mol^{-1}, which is smaller than those for the methoxycarbene ligands. The small allenylidene rotational barrier can be attributed to the small steric interaction between the aryl groups on the allenylidene ligand and the −Me groups on Me_3Tacn.

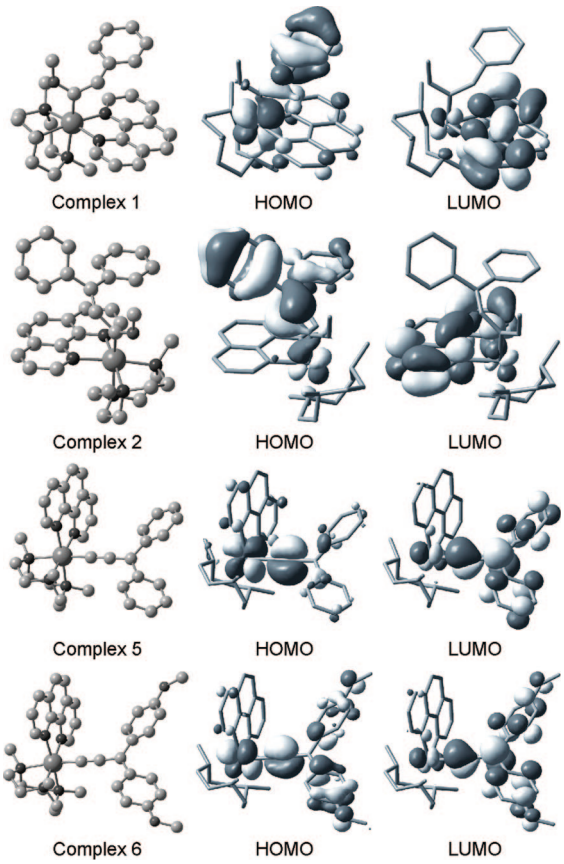

Figure 5. Optimized structures and HOMO and LUMO surfaces for complexes **1**, **2**, **5**, and **6** using the PBE1PBE functional (Ru−N_{Tacn} connectivities are omitted for clarity, surface isovalue = 0.03 au).

Conclusions

A series of ruthenium−methoxycarbene and −allenylidene complexes supported by the Me_3Tacn and phen ligands have been synthesized, and the ruthenium−methoxycarbene/allenylidene bonding interactions have been probed by spectroscopic and theoretical studies. The molecular structures of $\mathbf{1}(PF_6)_2\cdot(CH_3)_2CO$ and $\mathbf{2}(PF_6)_2\cdot(CH_3)_2CO$ have been characterized by X-ray crystallography. The lowest-energy absorption

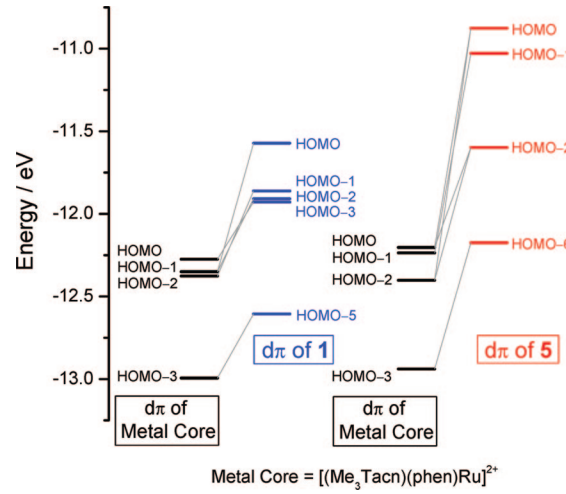

Figure 6. Plot of the energies of the d_π orbitals for the calculated complexes **1** and **5** and their corresponding frozen $[(Me_3Tacn)$-$(phen)Ru]^{2+}$ fragments.

Table 3. Charge Decomposition Analysis (CDA) for the $[(Me_3Tacn)(Phen)Ru]^{2+}$−L Interaction

L	L → M donation (*d*)	M → L back-donation (*b*)	*b*/*d*	repulsion (*r*)	residue (Δ)
:C(OMe)CH_2Ph	1.114	0.623	0.559	−0.784	−0.026
:C(OMe)CH═CPh_2	0.964	0.615	0.638	−0.821	−0.022
:C═C═CPh_2	1.636	0.518	0.317	−0.553	−0.042
:C═C═C(C_6H_4OMe-4)$_2$	1.678	0.468	0.279	−0.540	−0.047

Table 4. NBO Analysis for $[(Me_3Tacn)(Phen)Ru(L)]^{2+}$

	natural charge			
L	Ru	C_α	C_β	C_γ
:C(OMe)CH_2Ph	0.45	0.47		
:C(OMe)CH═CPh_2	0.45	0.44		
:C═C═CPh_2	0.41	0.04	−0.23	0.12
:C═C═C(C_6H_4OMe-4)$_2$	0.40	0.01	−0.24	0.10

bands for methoxycarbene complexes **1**−**4** and allenylidene complexes **5** and **6** are assigned as $d_\pi(Ru^{II}) \rightarrow \pi^*$(phen) MLCT and metal-perturbed $\pi \rightarrow \pi^*$ [Ru═C═C═CR_2] intraligand

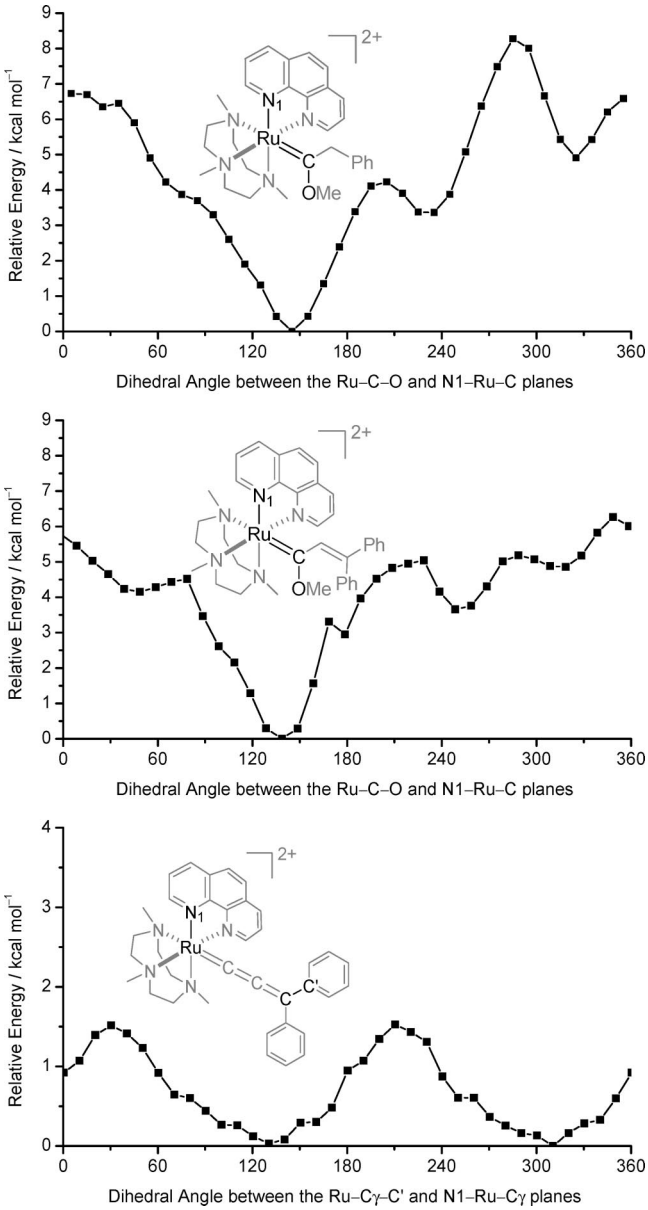

Figure 7. Plots of energy as a function of dihedral angles between the Ru−C_α−O and N(1)−Ru−C_α planes for complexes **1** and **2** and the angle between the Ru−C_γ−C′ and N(1)−Ru−C_γ planes for complex **5** (calculated in steps of 10°; energies are relative to their lowest-energy optimized structures).

transitions, respectively. The emissions of the methoxycarbene complexes at λ_{max} = 570−620 nm in glassy MeOH/EtOH solution at 77 K (λ_{ex} = 430 nm) are tentatively assigned as $d_\pi(Ru^{II}) \rightarrow \pi^*$(phen) ^{3}MLCT in nature. Theoretical calculations suggest that the Ru−C bonds in the allenylidene complexes are polarized in a $Ru^{\delta+}$═$C^{\delta-}$ manner, while the Ru−C bonds in the methoxycarbene complexes are nonpolarized in nature. Charge decomposition analysis suggests that allenylidene ligands are better electron donors and poorer electron acceptors compared with methoxycarbene ligands. The methoxycarbene/allenylidene rotational barriers on **1**, **2**, and **5** are calculated to be 8.3, 6.3, and 1.5 kcal mol^{-1}, respectively. This study suggests that the Ru−L bonding interaction has a dramatic effect on the optical properties of $[Ru(diimine)_x(L)_y]^{n+}$ (L = carbon-rich organic moieties), and functional emissive materials may be devised by tuning the Ru−L interaction. Work is in progress to synthesize derivatives with bulky aromatic diimine or carbene ligands; this would result in the formation of better functional emissive ruthenium(II)−carbene complexes.

Experimental Section

General Procedures. All reactions were performed under an argon atmosphere using standard Schlenk techniques unless otherwise stated. All reagents were used as received, and solvents were purified by standard methods. $[(Me_3Tacn)(phen)Ru(OH_2)](PF_6)_2$ was prepared according to a modified literature procedure for the synthesis of $[(Me_3Tacn)(2,2'\text{-bipyridine})Ru(OH_2)](ClO_4)_2$.[13] ^{1}H and $^{13}C\{^1H\}$ NMR spectra were recorded on Bruker 300/400/500 DRX FT-NMR spectrometers. Peak positions were calibrated with solvent residue peaks as internal standard. Electrospray mass spectrometry was performed on a PE-SCIEX API 3000 triple quadrupole mass spectrometer. Infrared spectra were recorded as KBr plates on a Perkin-Elmer FTIR-1600 spectrophotometer. UV−visible spectra were recorded on a Hewlett-Packard HP8452A diode array spectrophotometer interfaced with an IBM-compatible PC. Elemental analyses were done on an Elementar Vario EL analyzer.

Syntheses. $[(Me_3Tacn)(phen)Ru(OH_2)](PF_6)_2$. This is a modified literature procedure for the synthesis of $[(Me_3Tacn)(2,2'\text{-bipyridine})Ru(OH_2)](ClO_4)_2$.[13] A mixture of $Ru(Me_3Tacn)Cl_3$ (0.1 g, 0.26 mmol), 1,10-phenanthroline (phen) (0.05 g, 0.28 mmol), zinc powder (0.4 g, 6.15 mmol), and deionized water (40 mL) was refluxed for 1 h, during which the reaction mixture gradually turned reddish-brown. Upon cooling to room temperature, the mixture was filtered off under argon to remove the zinc powder. An aqueous solution of NH_4PF_6 (2 g, 12.27 mmol, in 3 mL of H_2O) was added to afford a red-brown precipitate (yield: 65%). This solid was used for the synthesis of complexes **1**−**6** without further characterization.

$[(Me_3Tacn)(phen)Ru$═$C(OMe)R](PF_6)_2$, 1−4$(PF_6)_2$. Excess HC≡CPh or HC≡CCR_2OH (0.7 mmol) was added to a methanolic solution (20 mL) containing $[(Me_3Tacn)(phen)Ru(OH_2)](PF_6)_2$ (0.15

(21) Auger, N.; Touchard, D.; Rigaut, S.; Halet, J.-F.; Saillard, J.-Y. *Organometallics* **2003**, *22*, 1638.
(22) Brady, M.; Weng, W.; Zhou, Y.; Seyler, J. W.; Amoroso, A. J.; Arif, A. M.; Böhme, M.; Frenking, G.; Gladysz, J. A. *J. Am. Chem. Soc.* **1997**, *119*, 775.
(23) (a) Schilling, B. E. R.; Hoffmann, R.; Lichtenberger, D. L. *J. Am. Chem. Soc.* **1979**, *101*, 585. (b) Kostić, N. M.; Fenske, R. F. *J. Am. Chem. Soc.* **1982**, *104*, 3879. (c) Kostić, N. M.; Fenske, R. F. *Organometallics* **1982**, *1*, 974.

g, 0.20 mmol). After refluxing for 12 h, the reaction mixture was concentrated and filtered off. The yellow or orange precipitates were washed with diethyl ether and dried under vacuum. The solid was then recrystallized by slow diffusion of Et_2O into an acetone solution to give bright yellow or orange crystals.

Complex 1(PF$_6$)$_2$ (R = CH$_2$Ph). Yield: 0.14 g, 80%. Anal. Calcd for $C_{30}H_{39}N_5ORuP_2F_{12}\cdot(CH_3)_2CO$: C, 42.34; H, 4.85; N, 7.49. Found: C, 42.28; H, 4.98; N, 7.62. ^{1}H NMR (500 MHz, $(CD_3)_2CO$): δ 1.48 (s, 3H, Me_3Tacn), 2.88−2.93, 3.30−3.41, 3.71−3.75 (m, 18H, Me_3Tacn), 3.65 (s, 2H, CH_2Ph), 4.67 (s, 3H, OMe), 6.05 (d, J = 7.2 Hz, 2H, Ph), 6.75−6.78 (m, 2H, Ph), 6.84−6.87 (m, 1H, Ph), 7.98 (dd, 2H, J = 8.1, 5.5 Hz, phen), 8.32 (s, 2H, phen), 8.84 (dd, 2H, J = 8.1, 1.1 Hz, phen), 9.31 (dd, 2H, J = 5.5, 1.1 Hz, phen). ^{13}C NMR (126 MHz, $(CD_3)_2CO$): δ 48.4, 56.4, 58.0, 62.2, 62.8, 63.3 (Me_3Tacn + OMe); 52.7 (CH_2Ph); 126.6, 127.1, 127.4, 129.2, 129.4, 131.2, 132.3, 139.3, 149.5, 155.0 (six from phen, four from Ph); 315.2 (Ru=C). IR (KBr, cm^{-1}): $\nu_{C=C/C=N}$ = 1463, 1629, ν_{P-F} = 840. ESI-MS: m/z 293 [M^{2+}], 731 [M^{2+} + PF$_6^-$].

Complex 2(PF$_6$)$_2$ (R = CH=CPh$_2$). Yield: 0.16 g, 83%. Anal. Calcd for $C_{37}H_{43}N_5ORuP_2F_{12}\cdot(CH_3)_2CO$: C, 46.91; H, 4.83; N, 6.84. Found: C, 46.85; H, 4.81; N, 6.90. ^{1}H NMR (300 MHz, $(CD_3)_2CO$): δ 1.41 (s, 3H, Me_3Tacn), 2.75−2.95, 3.20−3.45, 3.65−3.82, 3.85−4.03 (m, 18H, Me_3Tacn), 4.65 (s, 3H, OMe), 5.29 (s, 1H, −CH=CPh$_2$), 5.88 (d, J = 7.1 Hz, 2H, Ph), 6.29 (d, J = 7.1 Hz, 2H, Ph), 7.01 (m, 2H, Ph), 7.13 (m, 3H, Ph), 7.26 (m, 1H, Ph), 7.53 (m, 1H, phen H), 8.16−8.42 (m, 3H, phen H), 8.56 (d, J = 3.4 Hz, 1H, phen), 8.67 (d, J = 7.6 Hz, 1H, phen), 9.09 (d, J = 7.6 Hz, 1H, phen), 9.53 (d, J = 3.8 Hz, 1H, phen). ^{13}C NMR (75 MHz, $(CD_3)_2CO$): δ 48.9, 56.3, 57.0, 58.3, 58.8, 62.7, 62.8, 63.0, 64.4, 65.5 (Me_3Tacn + OMe); 127.2, 127.4, 129.3, 129.4, 129.5, 130.0, 130.3, 132.4, 136.7, 136.8, 137.5, 138.7, 139.7, 142.0, 155.0, 155.6 (phen + CH=CPh$_2$); 310.1 (Ru=C). IR (KBr, cm^{-1}): $\nu_{C=C/C=N}$ = 1468, 1628, ν_{P-F} = 840. ESI-MS: m/z 338 [M^{2+}], 820 [M^{2+} + PF$_6^-$].

Complex 3(PF$_6$)$_2$ (R = CH=C(C$_6$H$_4$Cl-4)$_2$). Yield: 0.16 g, 77%. Anal. Calcd for $C_{37}H_{41}N_5OCl_2RuP_2F_{12}\cdot(CH_3)_2CO$: C, 43.99; H, 4.34; N, 6.42. Found: C, 44.25; H, 4.68; N, 6.19. ^{1}H NMR (500 MHz, $(CD_3)_2CO$): δ 1.42 (s, 3H, Me_3Tacn), 2.85−2.88, 3.25−3.42, 3.68−3.74, 3.93−3.97 (m, 18H, Me_3Tacn), 4.67 (s, 3H, OMe), 5.49 (s, 1H, −CH=C(C$_6$H$_4$Cl-4)$_2$), 5.96 (d, J = 8.5 Hz, 2H, aryl H), 6.28 (d, J = 8.5 Hz, 2H, aryl H), 7.07 (d, J = 8.5 Hz, 2H, aryl H), 7.13 (d, J = 8.5 Hz, 2H, aryl H), 7.63−7.65 (m, 1H, phen), 8.24−8.37 (m, 3H, phen), 8.75−8.76 (m, 2H, phen), 9.09 (d, 1H, J = 8.0 Hz, phen), 9.55 (d, 1H, J = 5.1 Hz, phen). ^{13}C NMR (126 MHz, $(CD_3)_2CO$): δ 48.3, 55.8, 56.5, 57.7, 58.4, 62.1, 62.2, 62.5, 63.9, 65.1 (Me_3Tacn + OMe); 126.1, 127.0, 129.0, 129.2, 129.4, 129.7, 130.3, 130.8, 132.0, 132.5, 134.5, 134.6, 135.1, 136.2, 137.2, 139.4, 139.7, 148.9, 149.7, 154.5, 155.2 (phen + CH=C(C$_6$H$_4$Cl-4)$_2$); 308.1 (Ru=C). IR (KBr, cm^{-1}): $\nu_{C=C/C=N}$ = 1494, 1633, ν_{P-F} = 841. δ ESI-MS: m/z 372 [M^{2+}], 889 [M^{2+} + PF$_6^-$].

Complex 4(PF$_6$)$_2$ (R = CH=C(C$_6$H$_4$Me-4)$_2$). Yield: 0.15 g, 76%. Anal. Calcd for $C_{39}H_{47}N_5ORuP_2F_{12}\cdot(CH_3)_2CO$: C, 47.94; H, 5.08; N, 6.66. Found: C, 48.11; H, 5.00; N, 6.48. ^{1}H NMR (400 MHz, $(CD_3)_2CO$): δ 1.41 (s, 3H, Me_3Tacn), 2.19 (s, 3H, aryl Me), 2.32 (s, 3H, aryl Me), 2.75−2.95, 3.19−3.47, 3.65−3.81, 3.85−4.02 (m, 18H, Me_3Tacn), 4.64 (s, 3H, OMe), 5.25 (s, 1H, −CH=C(C$_6$H$_4$Me-4)$_2$), 5.82 (d, J = 7.9 Hz, 2H, aryl H), 6.16 (d, J = 7.8 Hz, 2H, aryl H), 6.83 (d, J = 7.7 Hz, 2H, aryl H), 6.90 (d, J = 7.8 Hz, 2H, aryl H), 7.50−7.62 (m, 1H, phen), 8.16−8.35 (m, 3H, phen), 8.58−8.73 (m, 2H, phen), 9.07 (d, J = 7.6 Hz, 1H, phen), 9.54 (d, J = 3.7 Hz, 1H, phen). ^{13}C NMR (101 MHz, $(CD_3)_2CO$): δ 20.9, 21.2 (Me on CH=C(C$_6$H$_4$Me-4)$_2$); 48.2, 55.6, 56.3, 57.6, 58.1, 62.0, 62.1, 62.3, 63.6, 64.6 (Me_3Tacn + OMe); 126.1, 126.6, 128.6, 128.9, 129.2, 130.1, 132.4, 134.9, 135.2, 137.0, 138.5, 138.7, 139.1, 139.5, 154.3, 154.8 (phen + CH=C(C$_6$H$_4$Me-4)$_2$); 309.7 (Ru=C). IR (KBr, cm^{-1}): $\nu_{C=C/C=N}$ = 1464, 1633, ν_{P-F} = 840. ESI-MS: m/z 352 [M^{2+}], 848 [M^{2+} + PF$_6^-$].

[(Me$_3$Tacn)(phen)Ru=C=C=CR$_2$](PF$_6$)$_2$, 5−6(PF$_6$)$_2$. Excess HC≡CCR$_2$OH (0.7 mmol) was added to a CH_2Cl_2 solution (20 mL) containing [(Me_3Tacn)(phen)Ru(OH$_2$)](PF$_6$)$_2$ (0.15 g, 0.20 mmol). After refluxing for 12 h, all solvent was removed under vacuum. The resultant deep purple (for **5**) or blue (for **6**) solid was washed with Et_2O (3 × 10 mL) and recrystallized by slow diffusion of Et_2O into an acetone solution to give bright purple or blue crystals. For the synthesis of **6**, MeOH can be used as solvent instead of CH_2Cl_2.

Complex 5(PF$_6$)$_2$ (R = Ph). Yield: 0.14 g, 75%. Anal. Calcd for $C_{36}H_{39}N_5RuP_2F_{12}$: C, 46.29; H, 4.21; N, 7.50. Found: C, 46.11; H, 4.20; N, 7.35. ^{1}H NMR (500 MHz, $(CD_3)_2CO$): δ 2.59 (s, 3H, Me_3Tacn), 3.26 (s, 6H, Me_3Tacn), 3.55−3.74, 3.98−4.03 (m, 12H, Me_3Tacn), 7.19−7.22 (m, 4H, H$_m$ of Ph), 7.37 (d, J = 8.4 Hz, 4H, H$_o$ of Ph), 7.73 (t, J = 7.5 Hz, 2H, H$_p$ of Ph), 8.17 (dd, 2H, J = 8.1, 5.5 Hz, phen), 8.49 (s, 2H, phen), 9.04 (dd, 2H, J = 8.1, 1.0 Hz, phen), 9.39 (dd, 2H, J = 5.5, 1.0 Hz, phen). ^{13}C NMR (126 MHz, $(CD_3)_2CO$): δ 50.7, 57.5, 60.4, 61.5, 64.0 (Me_3Tacn); 126.8, 129.4, 130.3, 130.5, 132.5, 140.4, 147.0, 149.3, 154.8, 155.0 (six from phen, four from aryl); 132.3 (C$_\gamma$); 158.4 (C$_\beta$); 309.1 (Ru=C). IR (KBr, cm^{-1}): $\nu_{C=C=C}$ = 1931, $\nu_{C=C/C=N}$ = 1426, 1459, 1628, ν_{P-F} = 840. ESI-MS: m/z 321 [M^{2+}], 788 [M^{2+} + PF$_6^-$].

Complex 6(PF$_6$)$_2$ (R = C$_6$H$_4$OMe-4). Yield: 0.17 g, 86%. Anal. Calcd for $C_{38}H_{43}N_5O_2RuP_2F_{12}$: C, 45.91; H, 4.36; N, 7.05. Found: C, 45.87; H, 4.48; N, 7.24. ^{1}H NMR (500 MHz, $(CD_3)_2CO$): δ 2.52 (s, 3H, Me_3Tacn), 3.29 (s, 6H, Me_3Tacn), 3.49−3.66, 3.86−3.90 (m, 18H, Me_3Tacn + OMe), 6.76 (d, J = 8.7 Hz, 4H, aryl), 7.34 (d, J = 8.5 Hz, 4H, aryl), 8.16 (dd, 2H, J = 8.1, 5.4 Hz, phen), 8.49 (s, 2H, phen), 9.01 (dd, 2H, J = 8.1, 0.8 Hz, phen), 9.48 (dd, 2H, J = 5.4, 0.8 Hz, phen). ^{13}C NMR (126 MHz, $(CD_3)_2CO$): δ 50.7 (OMe); 56.4, 57.2, 60.3, 61.3, 63.8 (Me_3Tacn); 115.8, 126.6, 129.3, 132.2, 133.7, 139.7, 149.5, 154.9, 155.0, 164.3 (six from phen, four from aryl); 139.4(C$_\gamma$); 158.0 (C$_\beta$); 292.3 (Ru=C). IR (KBr, cm^{-1}): $\nu_{C=C=C}$ = 1946, $\nu_{C=C/C=N}$ = 1427, 1463, 1592, 1633, ν_{P-F} = 840. ESI-MS: m/z 351 [M^{2+}], 848 [M^{2+} + PF$_6^-$].

X-ray Crystallography. The crystal data and details of data collection and refinement for **1**(PF$_6$)$_2$·(CH$_3$)$_2$CO and **2**(PF$_6$)$_2$·(CH$_3$)$_2$CO are summarized in the Supporting Information. A MAR diffractometer with a 300 mm image plate detector using graphite-monochromatized Mo Kα radiation (λ = 0.71073 Å) was employed for data collection. The images were interpreted and intensities integrated using the program DENZO,[24] and structures were solved by direct methods employing SIR-97[25] (for **1**(PF$_6$)$_2$·(CH$_3$)$_2$CO) and the SHELXS-97 program[26] (for **2**(PF$_6$)$_2$·(CH$_3$)$_2$CO) on a PC. The Ru and many non-H atoms were located according to the direct methods. The positions of the other non-hydrogen atoms were found after successful refinement by full-matrix least-squares using the program SHELXL-97[27] on a PC. In each complex, one crystallographic asymmetric unit consists of one formula unit. In the final stage of least-squares refinement, all non-hydrogen atoms were refined anisotropically (except the non-hydrogen atoms of acetone in **2**(PF$_6$)$_2$·(CH$_3$)$_2$CO) were refined isotropically). The positions of H atoms were calculated based on riding mode with thermal parameters equal to 1.2 times that of the associated C atoms and used in the calculation of final R-indices.

(24) *DENZO*: In Gewirth, D. *The HKL Manual, A description of programs DENZO, XDISPLAYF and SCALEPACK*; with the cooperation of the program authors Otwinowski, Z., and Minor, W.; Yale University: New Haven, CT, 1995.

(25) Altomare, A.; Burla, M. C.; Camalli, M.; Cascarano, G.; Giacovazzo, C.; Guagliardi, A.; Moliterni, A. G. G.; Polidori, G.; Spagna, R. *Sir97*: a new tool for crystal structure determination and refinement. *J. Appl. Crystallogr.* **1998**, *32*, 115.

(26) Sheldrick, G. M. *SHELXS97*, Programs for Crystal Structure Analysis (Release 97-2); University of Goetingen, Germany, 1997.

(27) Sheldrick, G. M. *SHELXL97*, Programs for Crystal Structure Analysis (Release 97-2); University of Goetingen: Germany, 1997.

Computational Methodology. Density functional theory (DFT) calculations were performed on complexes **1**, **2**, **5**, and **6**. Their electronic ground states were optimized without symmetry constraints using the density functional PBE1PBE,[17] which is a hybrid of the Perdew, Burke, and Ernzerhof exchange and correlation functional and 25% HF exchange. The Stuttgart small core relativistic effective core potentials were employed for Ru atoms with their accompanying basis sets.[28] The 6-31+G* basis set was employed for N, 6-31G* for C_α, and 6-31G for O and other C and H atoms.[29] Tight SCF convergence (10^{-8} au) was used for all calculations. Loose optimization convergence criteria (maximum step size of 0.01 au and an rms force of 0.0017 au) were used for the relaxed potential energy surface scan calculations. The nature of the Ru−C bonds was examined using charge decomposition analysis (CDA)[19] and natural bond orbital (NBO)[20] analysis. All the DFT calculations were performed using the Gaussian 03 program package (revision D.01),[30] while NBO and CDA analyses were performed with NBO 3.1[31] (implemented in Gaussian 03) and the QMForge program, respectively.[32]

Acknowledgment. The work described in this paper was supported by a grant from City University of Hong Kong (No. 7002302).

Supporting Information Available: Crystallographic information files (CIF) for $\mathbf{1}(PF_6)_2 \cdot (CH_3)_2CO$ and $\mathbf{2}(PF_6)_2 \cdot (CH_3)_2CO$; optimized geometries, orbital energies/compositions, and calculated frequencies for **1**, **2**, **5**, and **6**. This material is available free of charge via the Internet at http://pubs.acs.org.

OM800592A

(28) Andrae, D.; Haeussermann, U.; Dolg, M.; Stoll, H.; Preuss, H. *Theor. Chim. Acta* **1990**, *77*, 123.

(29) Hehre, W. J.; Ditchfield, R.; Pople, J. A. *J. Chem. Phys.* **1972**, *56*, 2257.

(30) Frisch, M. J.; Trucks, G. W.; Schlegel, H. B.; Scuseria, G. E.; Robb, M. A.; Cheeseman, J. R.; Montgomery, J. A., Jr.; Vreven, T.; Kudin, K. N.; Burant, J. C.; Millam, J. M.; Iyengar, S. S.; Tomasi, J.; Barone, V.; Mennucci, B.; Cossi, M.; Scalmani, G.; Rega, N.; Petersson, G. A.; Nakatsuji, H.; Hada, M.; Ehara, M.; Toyota, K.; Fukuda, R.; Hasegawa, J.; Ishida, M.; Nakajima, T.; Honda, Y.; Kitao, O.; Nakai, H.; Klene, M.; Li, X.; Knox, J. E.; Hratchian, H. P.; Cross, J. B.; Bakken, V.; Adamo, C.; Jaramillo, J.; Gomperts, R.; Stratmann, R. E.; Yazyev, O.; Austin, A. J.; Cammi, R.; Pomelli, C.; Ochterski, J. W.; Ayala, P. Y.; Morokuma, K.; Voth, G. A.; Salvador, P.; Dannenberg, J. J.; Zakrzewski, V. G.; Dapprich, S.; Daniels, A. D.; Strain, M. C.; Farkas, O.; Malick, D. K.; Rabuck, A. D.; Raghavachari, K.; Foresman, J. B.; Ortiz, J. V.; Cui, Q.; Baboul, A. G.; Clifford, S.; Cioslowski, J.; Stefanov, B. B.; Liu, G.; Liashenko, A.; Piskorz, P.; Komaromi, I.; Martin, R. L.; Fox, D. J.; Keith, T.; Al-Laham, M. A.; Peng, C. Y.; Nanayakkara, A.; Challacombe, M.; Gill, P. M. W.; Johnson, B.; Chen, W.; Wong, M. W.; Gonzalez, C.; Pople, J. A. *Gaussian 03, revision D.01*; Gaussian, Inc.: Wallingford, CT, 2004.

(31) Glendening, E. D.; Reed, A. E.; Carpenter, J. E.; Weinhold, F. *NBO 3.1*; Board of Regents of the University of Wisconsin System on behalf of the Theoretical Chemistry Institute, 1996−2004.

(32) (a) Tenderholt, A. L. *QMForge*, Version 2.1, http://qmforge.sourceforge.net. *QMForge* depends heavily on cclib, which does all the parsing and analysis. (b) O'Boyle, N. M.; Tenderholt, A. L.; Langner, K. M. *J. Comput. Chem.* **2008**, *29*, 839.